

# Numerical investigation on the seismic residual capacity of reinforced concrete beams' plastic hinges

Giulia Nicolò<sup>1</sup>, Livio Pedone<sup>1</sup>, Michele Matteoni<sup>1</sup>, Stefano Pampanin<sup>1</sup>

<sup>1</sup>Department of Structural and Geotechnical Engineering,  
Sapienza University of Rome,  
Via Eudossiana 18, 00184 Rome, Italy

## Abstract

This research work aims to investigate the seismic residual capacity of earthquake-damaged beams' plastic hinges, to support the decision-making in repair versus demolition. To this end, refined numerical models of reinforced concrete beams with different structural details are implemented in the finite element software DIANA. For each analysed configuration, capacity-reduction factors for stiffness ( $\lambda_k$ ), strength ( $\lambda_Q$ ), and deformation/ductility ( $\lambda_D$ ) are derived to simulate the effects of different damaging earthquakes. Results show that, even for a slight level of damage, a non-negligible reduction of plastic hinges' seismic capacity is observed, especially in terms of stiffness.

## 1 Background and motivations

Recent major earthquakes worldwide have further highlighted the urgency for an effective evaluation methodology of structures' seismic residual capacity. In fact, after an earthquake, buildings can be affected by substantial structural damage, which can lead to loss of their lateral-force resisting capacity. Yet, in the post-earthquake recovery phase, the lack of knowledge regarding the evaluation of the seismic performance of earthquake-damaged buildings could play a crucial role in the decision to demolish rather than repair/retrofit.

Considering, for instance, the 2010–2011 Canterbury earthquake sequence ([1], [2]), there is evidence that the main driving factors that led to the demolition of several damaged buildings were a lack of knowledge/guidelines in terms of: a) evaluation of the residual capacity of a damaged building to sustain subsequent aftershocks; b) selection and implementation of a set of reliable repairing techniques to bring back the structure to “at least” its as-is conditions before the earthquake; and c) the ability to predict the cost (or cost-effectiveness) of such a repair intervention, when compared to fully replacement costs and accounting for potential aftershock in the near futures [1],[4].

Moreover, in line with the “capacity design” philosophy (and contrary to the public's expectations), even up-to-date code-conforming structures can show significant structural damage when subjected to a design-level earthquake (e.g., Kam et al.[1]; Fig. 1). Therefore, proper and effective procedures for assessing the seismic residual capacity, including loss-assessment considerations and socio-economic impact evaluations, are needed for both existing structures and modern structures.



Fig. 1 Plastic hinges in the beams on the Precast 22-storey perimeter frame of the Price Waterhouse-Coopers PWC in Christchurch, New Zealand, after the 22<sup>nd</sup> Feb 2011 Christchurch Earthquake (adapted from Kam et al. [1]).

In the aftermath of an earthquake, the safety evaluation of buildings currently relies mainly on tagging procedures based on visual inspections (e.g., ATC [5], Baggio et al.[6]). Although these methodologies allow for a rapid safety evaluation of the damaged buildings, they are typically based only on expert judgment of the damage level. Yet, in addition to the visual inspection phase, a second phase employing a more refined safety assessment should be carried out through a Detailed Engineering Evaluation procedure (DEE, e.g. EAG 2012).

To this end, in the past decades, significant research efforts have been devoted to proposing seismic assessment methodologies for earthquake-damaged structures and specific guidelines have been developed (e.g., FEMA 306 [7], FEMA 307 [8], JBDPA guidelines [9][9]). Among others, in the FEMA 306 report capacity reduction factors for stiffness, strength, and ductility capacity (namely  $\lambda_K$ ,  $\lambda_Q$ , and  $\lambda_D$ , respectively) are proposed in order to account for the effects of a damaging earthquake on structural components. However, these guidelines are mainly focused on reinforced concrete (RC) and masonry wall structures. On the other hand, considering RC frame structures, only a few works in the literature investigated the residual capacity of structural components such as beam/column plastic hinges and beam-column joints (e.g., Di Ludovico et al.[10]; Cuevas and Pampanin[11]; Marder et al.[12]). Thus, research effort is still needed to evaluate the effects of earthquake-related damage to these structural components.

Considering the previous background, this paper aims to numerically investigate the seismic residual capacity of earthquake-damaged beams, characterized by either code-conforming or dated structural detailing. In line with the FEMA 306 approach, the goal of this research is to derive capacity-reduction factors for stiffness ( $\lambda_K$ ), deformation/displacement ( $\lambda_D$ ), and strength ( $\lambda_Q$ ) of damaged beam components. To this end, a parametric analysis is performed by implementing refined numerical models of RC beams with different structural details in the finite element software DIANA [13]. For each analysed configuration, the aforementioned capacity-reduction factors are derived by comparing the force-displacement capacity curve of the “as-built” and damaged configuration. Moreover, simplified regression-based relationships are also proposed to derive  $\lambda$ -factors as a function of the rotational ductility, in analogy with past studies in the literature (e.g., Di Ludovico et al.[10]).

## 2 Parametric investigation on RC beams

A parametric analysis is carried out to investigate the seismic residual capacity of RC beams. Detailed information about the implemented methodology and the analysis results are reported in this section.

### 2.1 RC beam configurations and modelling approach

The case-study beams are selected from experimental tests available in the literature. These beams are characterized by different structural details and plastic hinge developments (e.g., widespread cracks vs. single wide crack failure). The geometrical details and material properties of these RC beams are listed in Table 1. More details about the specimens can be found in the cited papers.

Table 1 Geometrical details and material properties of these RC beams (note:  $f_{ck}$  = concrete compression strength - characteristic value ;  $f_{yk}$  = steel yield stress-characteristic value ;  $\rho_l$  = longitudinal reinforcement ratio;  $\rho_w$  = transversal reinforcement ratio per metre).

Authors	ID	Section	Length [m]	$f_{ck}$ [MPa]	$f_{yk}$ [MPa]	$\rho_l$ [-]	$\rho_w$ [-]
Marder et al. [12]	CYC	720x320mm	2.750	30	300	0.006	0.01
Opabola et al. [21]	CYC-1.96.25	700x400mm	2.135	25	300	0.008	0.004

Each selected beam is analysed by implementing a refined FEM model in the structural software DIANA (DISplacement ANALyzer)[13]. Specifically, the adopted modelling approach consists of a two-dimensional (2D) numerical model. Concrete elements are modelled by plane stress regular elements, while steel reinforcements are modelled as ‘line’ elements embedded in the concrete beam. In

particular, every layer of reinforcement is modelled through one bar: the cross-section assigned to this bar is the sum of all the steel corresponding to that layer.

The concrete behaviour is modelled by the “Total strain crack model”, provided by the software. The constitutive model, based on total strain, relies on the Modified Compression Field Theory, originally proposed by Vecchio & Collins [14]. Similarly to the multi-directional fixed crack model, the total strain-based crack models follow a smeared approach for the fracture energy. In particular, the adopted approach is the “rotating crack model”, where the crack directions continuously rotate according to the strain vector's principal directions. The implemented concrete compressive behaviour is a parabolic relationship according to Feenstra's formulation [15], while the tensile behaviour is that proposed by Hordjik [16]. All the parameters required by the software have been selected according to the *fib* Model Code 2010 [17].

In order to implement non-linear cyclic analyses, the steel rebars are modelled using the Monti-Nuti constitutive law [18]. The relationship's parameters are defined according to the experimental behaviour of the bars (when available), while the loading-unloading constants are selected according to the ranges of values provided by Fragiadakis et al. [19]. Specifically, for the initial curvature  $R_0$  a value of 20 is assumed, the weighting parameter  $P$  is taken equal to 0.9 and the material constants  $A_1$  and  $A_2$  are assumed equal to 18.5 and 0.1 respectively. Moreover, it is worth mentioning that these models account for both materials and geometrical nonlinearities.

The numerical models are calibrated and validated by comparison with the available experimental results. In Fig. 2, an example of numerical vs. experimental results is reported for the specimen tested by Opabola et al. [20]. A good agreement between numerical and experimental behaviour is observed, confirming the reliability of the adopted modelling approach.

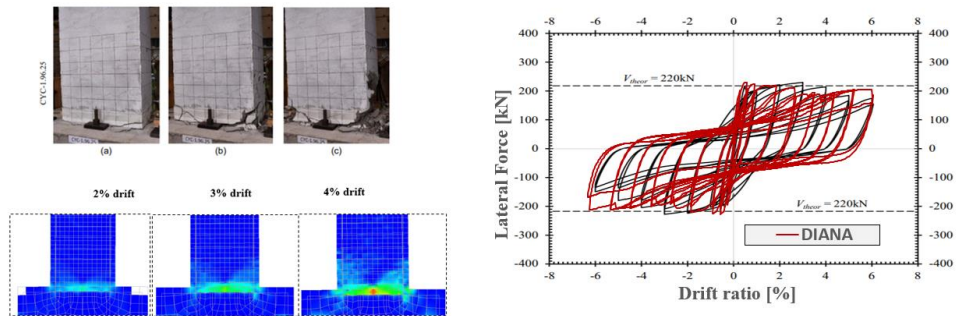


Fig. 2 Example of numerical vs. experimental results: (left) comparison in terms of observed crack patterns; (right) comparison in terms of non-linear cyclic response.

In order to increase the dataset, parametric configurations of the RC beams listed in Table 1 are defined and additional numerical models are implemented adopting the same modelling approach. The selected specimens allow for the definition of two different groups for the analysed beams, namely “Type-A” and “Type-B”. More specifically, Type-A beams rely on the experimental test performed by Marder et al. [21]. These RC beams are representative of typical cast-in-situ seismically-designed components. Accordingly, these beams present symmetrical longitudinal reinforcement and denser stirrups in the plastic hinge regions; deformed bars are used.

On the other hand, Type-B beams rely on the experimental test performed by Opabola et al. [20]. These beams are representative of components of modern designed buildings, but they are expected to show a different failure mechanism than Type-A beams. Specifically, due to the presence of curtailed bars (i.e., bars which are cut at the beam-joint interface), the development of a single crack instead of a distributed cracking is expected (e.g., Opabola et al. [20]). For each analysed beam typology (i.e., Type-A and Type-B) twelve parametric configurations are identified by modifying the structural details and geometrical features of the original specimens.

Additionally, a third beam typology is also investigated in this study, namely “Type-C”. Beams belonging to the Type-C typology are representative of non-seismic-code-conforming beams (e.g. pre-1970s existing structures in Italy) with typical inadequate structural details and deficiencies. In fact, these elements are designed for gravity loads only (e.g., with reinforcement bars disposed

asymmetrically in the section), and sections are lightly confined because of the wider spacing between the stirrups in the plastic hinge regions. In the group of Type-C beams twelve parametric configurations are defined.

Therefore, in total 36 beams with different structural details and expected failure mechanisms are analysed. Geometrical and construction details of the analysed configurations are listed in Table 2 and shown in Fig. 3.

Table 2 Geometrical details and material characteristics of the analysed configurations.

	d' (cover) [mm]	f <sup>'c</sup> [MPa]	f <sub>y</sub> [MPa]	s (stir. spacing) [mm]	BxH [mm]	Length [mm]
Type-A	35	40	300	120	300x500, 300x600, 300x700, 400x700	3000/5000/6000
Type-B	35	25	300	120	300x500, 300x600, 300x700, 400x700	3000/5000/6000
Type-C	25	25	300	200	300x500, 300x600, 300x700, 400x700	3000/5000/6000

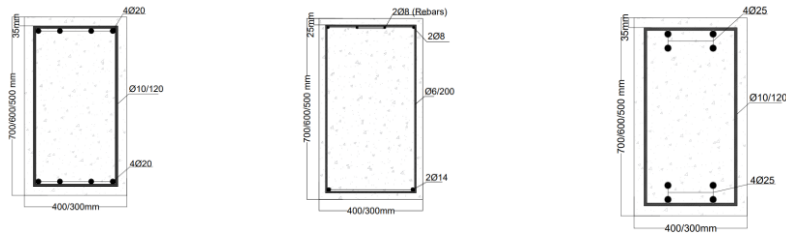


Fig. 3 (Left) Type-A (code-conforming beams), (Centre) Type-C (non-code-conforming beams), and (Right) Type-B (single crack beams).

## 2.2 Non-linear static analyses and $\lambda$ -factors evaluations

According to the FEMA 306 report [7], the most reliable approach to determine  $\lambda$ -factors would involve experimental investigations on two identical specimens for the analysed structural component. The first specimen would represent the component in its “intact” or “as-is” (i.e., pre-earthquake) configuration, while the second one would represent the component in its damaged (i.e., post-earthquake) configuration. Thus, by comparing the force-displacement capacity curves of the two specimens the capacity reductions factor would be carried out. Nevertheless, the FEMA 307 report [8] (which includes some theoretical information about the FEMA 306 report) points out that at the date of the document, these types of experimental tests were not available and, therefore, the  $\lambda$ -factors were rather derived considering individual cyclic-static tests.

In line with the FEMA 307 approach and similarly to past research work in the literature (e.g., Ceccarelli et al. [22]), the refined FEM models are subjected to two different loading protocols. The aim is to compare the seismic performance of the damaged components against the undamaged ones. Thus, the  $\lambda$ -factors can be derived by comparing the force-displacement curves of the damaged and undamaged components in terms of strength, stiffness, and displacement ductility. For each specimen, five different displacement ductility targets are considered for the derivation of the capacity-reduction factors.

To this end, each analysed beam is subjected to two different loading protocols, defined as follows:

- Unidirectional monotonic lateral load until failure, to evaluate the force-displacement capacity curve of the beam in its pre-event (i.e., undamaged) conditions.

- Quasi-static cyclic load until a target displacement ductility followed by unidirectional monotonic lateral load until failure, to evaluate the force-displacement capacity curve of the beam in its post-event (i.e., damaged) conditions. This procedure is repeated for each considered displacement-ductility (damage level) target. Specifically, each loading protocol is composed of three drift levels, and for each drift level, three complete cycles are performed (Fig. 4). The last considered drift level represents the displacement-ductility target.

In order to compare the force-displacement capacity curves of the undamaged and damaged configurations, the obtained non-linear curves are firstly bi-linearised. Three alternative bi-linearisation methods are considered in this study to account for the different assumptions on the definition of the yielding displacement (which may affect the results in terms of  $\lambda$ -factors). The used bi-linearisation methods are those suggested by the FEMA 273 [23], Paulay & Priestley [24] and NTC2018[25]. After the bi-linearization process, the non-linear curves are compared to derive the reduction factors in terms of stiffness, strength, and deformation limit (Fig. 4).

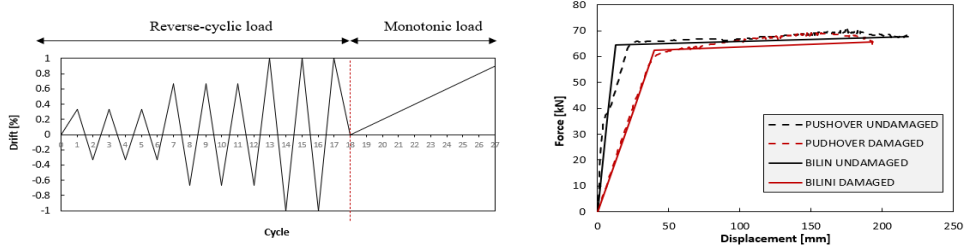


Fig. 4 (Left) Example of loading protocol, (Right) assessment of the reduction factors by comparing the damaged and the undamaged curves (FEMA 273 bilinearization).

The obtained  $\lambda$ -factors are computed and, for each analysed beam typology, are collected in diagrams as a function of the rotational ductility demand. These data are also used to derive simplified data-driven relationships for the evaluation of capacity reduction factors as a function of the rotation ductility demand (similar to Di Ludovico et al. [10]). To this end, the Ordinary Least Squares (OLS) regression method is implemented for the fitting of the data.

Detailed information on the results in terms of  $\lambda$ -factors and corresponding relationships is provided in the next paragraph.

### 3 Results and Discussion

In this section, the obtained  $\lambda$ -factors and the corresponding proposed analytical expression are presented. Results in terms of  $\lambda$ -factors for each analysed beam typology are shown in Fig.5, while the obtained regression-based formulations are listed in Table 3, together with the observed coefficient of determinations ( $R^2$ ).

Table 3 Regression equations for the  $\lambda$ -factors

Type-A (code-conforming beams)	Type-B (single crack beams)	Type-C (non-code-conforming beams)
$\lambda_k = 1$ for $\mu_\theta \leq 1$ $\lambda_k = \mu_\theta^{-1.535}$ for $1 \leq \mu_\theta \leq 10.64$ $R^2 = 0.439$	$\lambda_k = 1$ for $\mu_\theta \leq 1$ $\lambda_k = \mu_\theta^{-1.743}$ for $1 \leq \mu_\theta \leq 7.24$ $R^2 = 0.39$	$\lambda_k = 1$ for $\mu_\theta \leq 1$ $\lambda_k = 0.99\mu_\theta^{-2.97}$ for $1 \leq \mu_\theta \leq 9.68$ $R^2 = 0.83$
$\lambda_Q = 1$ for $\mu_\theta \leq 5.5$ $\lambda_Q = -0.093\mu_\theta + 1.516$ for $5.5 \leq \mu_\theta \leq 10.64$ $R^2 = 0.94$	$\lambda_Q = 1$ for $\mu_\theta \leq 2.68$ $\lambda_Q = -0.212\mu_\theta + 1.568$ for $2.68 \leq \mu_\theta \leq 7.24$ $R^2 = 0.49$	$\lambda_Q = 1$ for $\mu_\theta \leq 1$ $\lambda_Q = 0.992\mu_\theta^{-0.382}$ for $1 \leq \mu_\theta \leq 9.68$ $R^2 = 0.73$
$\lambda_D = 1$ for $\mu_\theta \leq 2.02$ $\lambda_D = 1.35\mu_\theta^{-0.43}$ for $2.02 \leq \mu_\theta \leq 0.64$ $R^2 = 0.61$	$\lambda_D = 1$ for $\mu_\theta \leq 1.67$ $\lambda_D = 1.52\mu_\theta^{-0.82}$ for $1.67 \leq \mu_\theta \leq 7.24$ $R^2 = 0.67$	$\lambda_D = 1$ for $\mu_\theta = 1$ $\lambda_D = \mu_\theta^{-0.117}$ for $1 \leq \mu_\theta \leq 9.68$ $R^2 = 0.86$

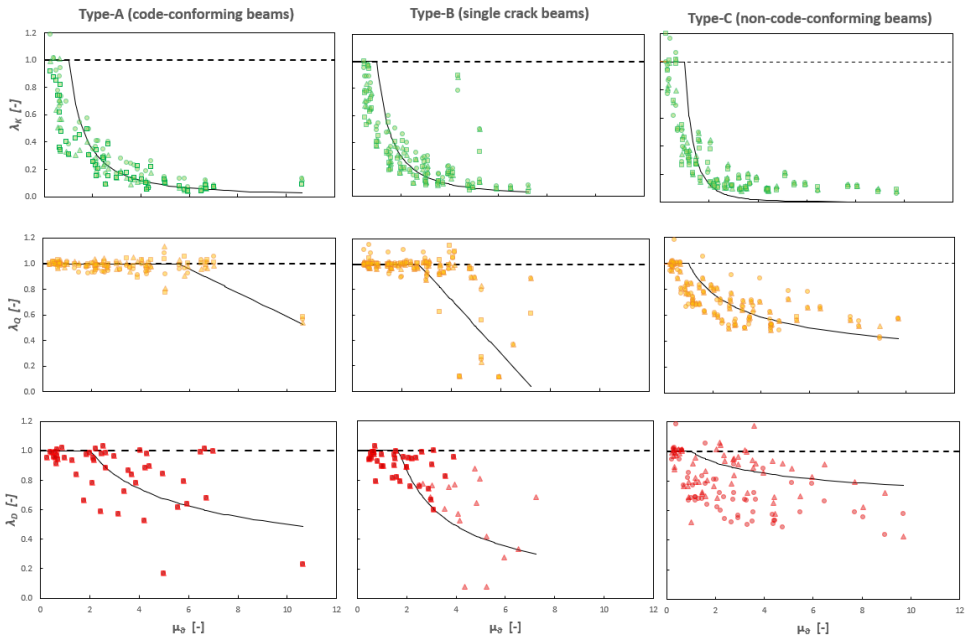


Fig. 5 Reduction factors ( $\lambda$ ) and corresponding regression-based relationships.

It is worth mentioning that the values obtained for a rotation ductility minor than 1 (which should represent an elastic behaviour) have been neglected in the regression analysis. This choice is made since these values correspond to a loss of capacity due to the concrete cover cracking, which is typically neglected in numerical simulations implemented in engineering practice. In other words, the effects of concrete cracking are typically already accounted for in non-linear numerical models based on a lumped plasticity approach (widely adopted in the current practice) by considering an effective stiffness secant to the yielding point. For these reasons, the proposed formulations should be considered representative of the effect of damage due to only plastic deformation. Results show that, as expected, stiffness is the most sensitive parameter with damage. In the case of non-code-conforming beams (Type-C), a different trend for strength reduction factors ( $\lambda_Q$ ) is observed when compared with Type-A and Type-B beams. Specifically, a severe reduction in terms of strength capacity is observed even for low ductility levels. A lower dispersion in the results is also obtained if compared to the  $\lambda_Q$ -values of the other two beam typologies (i.e., Type-A, Type-B). However, for the latter, strength degradation starts for higher ductility levels and the trend of the curves is affected by a significant dispersion. High dispersion in the results is also observed for the ductility reduction factors  $\lambda_D$ . It is worth noting that in some cases there are  $\lambda$  values that are over 100%, which are physically unsound. This result is mainly due to the adopted bilinearization method.

The results are finally compared with those proposed by Di Ludovico et al. [10] for non-code-conforming columns and those proposed by Marder et al. [12] for code-conforming beams (Fig. 6). As shown in Fig. 6, results in terms of stiffness reduction  $\lambda_k$  are in good agreement with both the results of Di Ludovico et al. [10] and Marder et al. [12] in terms of observed shapes. However, the proposed formulations highlight a higher loss of stiffness (at the same ductility level) for the analysed beams when compared to the relationships for columns. As far as the strength capacity reduction factor  $\lambda_Q$  is concerned, the formulation proposed by Di Ludovico et al. is similar only to the observed trend for Type-A beams (modern beams). This difference is most likely expected and given to the different types of structural components analysed, i.e. columns rather than beams, as well as to the non-negligible dispersion in both results.

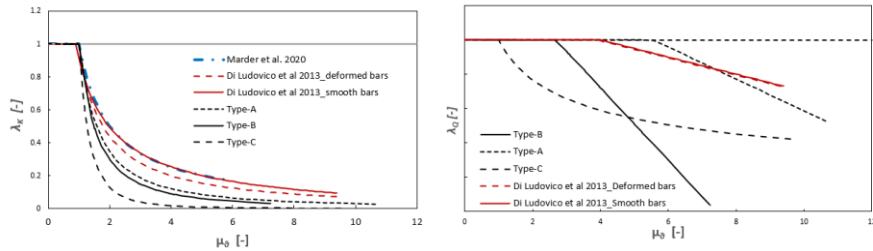


Fig. 6 Comparison of reduction factors vs. drift-ductility level (pre-damage) with literature results on columns and beams. (Left) stiffness reduction factor  $\lambda_K$ ; (Right) strength reduction factor  $\lambda_Q$ .

## 4 Conclusions

A numerical investigation on the seismic residual capacity of beams' plastic hinges has been presented. In line with the FEMA 306 approach, originally focused on wall elements, the work aimed to derive simplified data-driven relationships for evaluating capacity reduction factors for beam plastic hinges in terms of stiffness, strength, and deformation limits (namely,  $\lambda_K$ ,  $\lambda_Q$ , and  $\lambda_D$ , respectively). To this end, a parametric analysis of different beams characterized by different structural details and expected failure modes has been performed. Each beam has been analyzed through a refined numerical model implemented in the structural software DIANA. Capacity reduction factors have been carried out by comparing the force-displacement capacity curves of the pre- and post-earthquake (i.e., undamaged and earthquake-damaged) configurations.

The main observation can be summarised as follows:

- Stiffness is the most sensitive parameter to damage, confirming the observations of past studies available in the literature;
- The adopted bi-linearization methods may strongly affect the results in terms of capacity-reduction factors. Moreover, in some cases,  $\lambda$  values higher than 100% are observed, and this inconsistent result is deemed to be due to the adopted bi-linearization method;
- Higher dispersion is observed for ductility ( $\lambda_D$ ) and strength ( $\lambda_Q$ ) capacity reduction factors;
- By comparing the obtained results in terms of observed trends for  $\lambda$ -factors with other results available in the literature [26], a good agreement has been observed for stiffness reduction factors ( $\lambda_K$ ).

Results presented in this study can be used to perform seismic risk analyses in post-earthquake conditions, directly accounting for the effect of cumulative damage. Nevertheless, future experimental investigations are needed to better validate the presented result.

## References

- [1] Kam, Weng Y., Stefano Pampanin, Rajesh Dhakal, Henri P. Gavin, and Charles Roeder. 2010. "Seismic performance of reinforced concrete buildings in the September 2010 Darfield (Canterbury) earthquake". *Bulletin of the New Zealand Society for Earthquake Engineering*. 43, 340-350.
- [2] Kam, Weng Y., Stefano Pampanin, and Ken Elwood. 2011. "Seismic performance of reinforced concrete buildings in the 22 February Christchurch (Lyttelton) earthquake." *Bulletin of the New Zealand Society for Earthquake Engineering*. 44, 239–278
- [3] Pampanin, Stefano, Alberto Cuevas, Milo Kral, Giuseppe Loporcaro, Allan Scott, and Amir Malek. 2015. "Residual capacity and repairing options for reinforced concrete buildings". Research Report Prepared for the Natural Hazard Research Platform, University of Canterbury.
- [4] Marquis, Frederic, Jenna J. Kim, Kenneth. J. Elwood, and Stephanie E. Chang. 2017. "Understanding post-earthquake decisions on multi-storey concrete buildings in Christchurch, New Zealand." *Bulletin of Earthquake Engineering*, 15, 731-758
- [5] Applied Technology Council. 1996. "Seismic evaluation and retrofit of concrete buildings." Volume 1. Technical Report. Redwood City, California, USA.
- [6] Baggio, Carlo, Alberto Bernardini, Riccardo Colozza, Livio Corazza, Marianna Della Bella, Giacomo Di Pasquale, Mauro Dolce, Agostino Goretti, Antonio Martinelli, Giampiero Orsini,



- Filomena Papa, and Giulio Zuccaro. 2007. "Field Manual for Post-Earthquake Damage and Safety Assessment and Short Term Countermeasures (AeDES)." JRC, Ispra, Italy
- [7] Federal Emergency Management Agency (FEMA). 1998.FEMA." Evaluation of Earthquake Damaged Concrete and Masonry Wall Buildings – Basic procedures manual." FEMA 306 report, Washington DC, USA.
- [8] Federal Emergency Management Agency (FEMA).1998." Evaluation of Earthquake Damaged Concrete and Masonry Wall Buildings – Technical Resources." FEMA 307 report, Washington DC, USA.
- [9] The Japan Building Disaster Prevention Association (JBDPA).1991. "Guideline for Post-earthquake Damage Evaluation and Rehabilitation"
- [10] Di Ludovico, Marco, Maria Polese, Marco Gaetani d’Aragona, Andrea Prota, and Gaetano Manfredi. 2013."A proposal for plastic hinges modification factors for damaged RC columns." *Eng Struct* 51:99–112. DOI: [10.1016/j.engstruct.2013.01.009](https://doi.org/10.1016/j.engstruct.2013.01.009)
- [11] Cuevas, Alberto, and Stefano Pampanin. 2014. "Accounting for residual capacity of reinforced concrete plastic hinges: current practice and proposed framework". 2014 NZSEE Conference.
- [12] Marder, Kai, Kenneth J. Elwood, Christopher J. Motter, and Charles G. Clifton. 2020."Post-earthquake assessment of moderately damaged reinforced concrete plastic hinges". *Earthquake Spectra*, 36(1), 299–321.
- [13] TNO DIANA, DIANA, T. 2019. "Finite element analysis user’s manual: Release 10.3", Netherlands.
- [14] Vecchio, Frank J., and Michael P. Collins.1986. "The Modified Compression Field Theory for Reinforced Concrete subjected to Shear". *ACI Journal*, Proceedings V. 83, No. 2, Mar.-Apr. 1986
- [15] Feenstra, Peter H. 1993." Computational Aspects of Biaxial Stress in Plain and Reinforced Concrete." PhD diss., Delft University of Technology
- [16] Cornelissen, Hans A. W., Dirk A. Hordijk, and Hans W. Reinhardt. 1986. "Experimental determination of crack softening characteristics of normalweight and lightweight concrete". *Heron* 31 (2)
- [17] *fib Model Code 2010, Vol. 1, Bull. 65*; International Federation for Structural Concrete: Lausanne, Switzerland, 2012.
- [18] Monti, Giorgio and Camillo Nuti. 1992. "Nonlinear cyclic behaviour of reinforcing bars including buckling." *J. Struct. Eng.* 118(12): 3268-3284
- [19] Fragiadakis, Michalis, Rui Pinho, and Stelios Antoniou. 2008. "Modelling inelastic buckling of reinforcing bars under earthquake loading". *Computational Structural Dynamics and Earthquake Engineering* pp. 347–361 <https://doi.org/10.1201/9780203881637.ch22>
- [20] Opabola, Eytayo A., and Kenneth J. Elwood. 2023. "Seismic Performance of Reinforced Concrete Beams Susceptible to Single-Crack Plastic Hinge Behavior." *Journal of Structural Engineering* 149(4) <https://doi.org/10.1061/jsendh.steng-11424>
- [21] Marder, Kai, Christopher Motter, Kenneth J. Elwood, and Charles G. Clifton. 2018. "Testing of 17 identical ductile reinforced concrete beams with various loading protocols and boundary conditions". *Earthquake Spectra*, 34(3), 1025-1049.
- [22] Ceccarelli, Cristiana, Simona Bianchi, Livio Pedone, and Stefano Pampanin. 2021."Numerical Investigations on the Residual Capacity and Economic Losses of Earthquake-Damaged Reinforced Concrete Wall Structures." Proceedings of the 8th Annual Conference on Computational Methods in Structural Dynamics and Earthquake Engineering Methods in Structural Dynamics and Earthquake Engineering
- [23] Federal Emergency Management Agency (FEMA).1997. NEHRP Guidelines for Seismic Rehabilitation of Buildings. FEMA-273, Building Seismic Safety Council, Washington, D.C.
- [24] Paulay, Tom, and Nigel M.J. Priestley.1992. "Seismic design of reinforced concrete and masonry buildings". Wiley, New York.
- [25] Ministero delle infrastrutture e dei trasporti. 2018. *Aggiornamento delle Norme tecniche per le costruzioni. Gazzetta Ufficiale Serie Generale* 42. Rome, Italy.
- [26] Pampanin, Stefano. 2021. "Simplified Analytical/Mechanical Procedure for Post-earthquake Safety Evaluation and Loss Assessment of Buildings". *Springer Tracts in Civil Engineering*, 3–25. DOI:[10.1007/978-3-030-68813-4\\_1](https://doi.org/10.1007/978-3-030-68813-4_1)